Available online at www.sciencedirect.com
ScienceDirect
IFAC PapersOnLine 59-32 (2025) 114–119

Developing a Communication Node Deployment System for UGVs ⋆

C. Fisher * **MJ. McDermott** **

* *The Department of Electrical and Electronic Engineering, Stellenbosch University. (e-mail: cfisher@sun.ac.za)*
** *The Department of Electrical and Electronic Engineering, Stellenbosch University. (e-mail: 24803472@sun.ac.za).*

Abstract:
This paper presents the development of a modular proof-of-concept system capable of autonomously deploying communication nodes from Unmanned Ground Vehicles (UGVs). This enables the establishment of a temporary mesh communication network for hazardous environments, such as subterranean mines and during Search-and-Rescue (SAR) deployments. A prototype system was developed to facilitate the storage and deployment of two distinct types of self-righting communication nodes, each offering unique advantages and disadvantages. The system was designed to be modular, enabling multiple storage units to be stacked to meet the required number of nodes for a particular mission. Experimental testing demonstrated the system's potential for further development to enhance it's robustness against the harsh environments encountered in SAR applications and subterranean mining.

Keywords: Deployment Mechanism, Communication Node, Sensor Node, Breadcrumb, Mesh Network, Self-Righting Mechanism, Search-and-Rescue, Subterranean Mining

1. INTRODUCTION

During disaster events or emergency SAR missions, the deployment of robotic platforms can be critical in preserving life and preventing further casualties by reducing risk to rescue teams. Subterranean environments, such as underground mines, present unique challenges and are particularly hazardous for humans, especially during a disaster situation. Moreover, according to Cruz-Ausejo et al. (2024), 8 % of global occupational fatalities occur in the mining sector, which employs only 1 % of the global workforce. Many of these fatalities are attributed to hazards such as toxic gas leaks, tunnel collapses, ionising radiation exposure, and poor air quality (Cruz-Ausejo et al., 2024). Therefore, the deployment of robotic platforms enables safer route planning for rescue operations. However, one of the primary limitations in these environments is the absence of established communication networks to support robotic platforms. Several approaches can be considered to address this issue, including the use of fully autonomous robots, tethered robots, or the deployment of communication networks.

In underground mines, a fibre optic backbone coupled with limited Wi-Fi connectivity typically exists. However, this connectivity does not extend to the stope face, and during disasters, it is often the first infrastructure to fail due to severed cables or loss of power, rendering it unreliable. These environments are extremely rough and hazardous for both robots and humans. Although fully autonomous robots could provide a solution, the absence of communication prevents real-time data acquisition, requiring the robot to return before any information can be retrieved. However, delays in return introduce uncertainties regarding whether the robot is immobilised, lost, or still exploring. Furthermore, the use of tethered robots presents operational limitations due to the small search spaces, typically less than 200 metres, and the possibility of the fibre optic tether becoming snagged or severed by objects in hazardous environments. Therefore, an optimal solution is the development of an autonomous or teleoperated robotic platform capable of deploying a wireless mesh network, thereby establishing communication links, expanding the effective search area, and enabling live data acquisition.

2. BACKGROUND

In 2017, Defense Advanced Research Projects Agency (DARPA) created the Subterranean (SubT) challenge to incentivise research teams to develop autonomous and teleoperated robotic systems to map, navigate, and explore complex underground networks. Node deployment systems were employed to dispense communication nodes (breadcrumbs) at determined locations, thereby extending network coverage and establishing communication during exploration. Fig. 1 illustrates an example of such a network architecture.

However, one of the main limitations in establishing communication networks in subterranean environments is determining the optimal placement of each node. Tranzatto et al. (2022a) referred to Team Explorer's approach, in which cost functions were calculated by considering variables such as distance, line-of-sight, and Received Signal Strength Indicator (RSSI) conditions to determine when

⋆ The authors would like to thank Enaex Africa for funding this work.

10.1016/j.ifacol.2025.12.406

to deploy a node. Additionally, Tatum (2020) developed a predictive mapping algorithm to optimise communication coverage. Although these solutions offer advantages, some teams found them to be computationally expensive and considered advanced autonomous navigation without communication more suitable. In such cases, a single off-the-shelf communication node functioned as a base station, allowing robots to rendezvous and relay information for off-board processing.

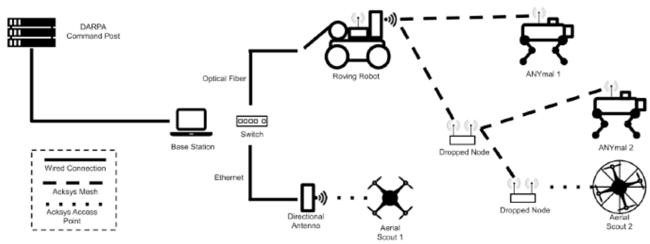

Fig. 1. Team CERBERUS Network Architecture (Tranzatto et al., 2022a).

Developing advanced autonomous navigation and exploration algorithms is beneficial for robotics in general, however, it presents major limitations for SAR applications, as there is no real-time information available for the rescue team. Therefore, if a robot locates someone in need, there is a significant delay before that information reaches the rescue team as the robot has to navigate back to the base station. If no information is received, then it either indicates that the robot has seen nothing of concern and is still exploring, or something has gone wrong and the robot cannot make it back to the base station. This highlights the need for a deployable mesh network to enable real-time communication with the robot.

Additionally, recent research into military applications of both autonomous and tethered control of Unmanned Ground Vehicles (UGVs) highlights the critical challenge of maintaining reliable communication in remote environments. Candido et al. (2025) emphasises that "backup radio communication is essential in remote areas without mobile networks." This further reinforces the importance of equipping UGVs with the ability to store and deploy communication nodes (breadcrumbs) to establish ad hoc mesh networks when conventional network infrastructure is unavailable or disrupted.

However, a major limitation of deploying communication nodes is ensuring that the antennas are correctly oriented after deployment. If the antennas are misaligned, attenuation occurs due to polarization mismatch, rendering the node ineffective, as detailed in Section 2.1. Several teams that developed custom breadcrumbs adopted the approach of incorporating a spring mechanism to automatically actuate the antenna upright upon deployment. Fig. 2 depicts the spring-loaded breadcrumb designs developed by Team CERBERUS and CSIRO Data61. Since the focus of the DARPA Subterranean Challenge was on autonomous exploration and mapping of complex subterranean environments, the specific details regarding the development of the communication nodes and their respective deployment systems were not disclosed. However, based on the figures and brief functional explanations provided, certain assumptions can be made to assist in selecting the design specifications discussed in Section 3.1.

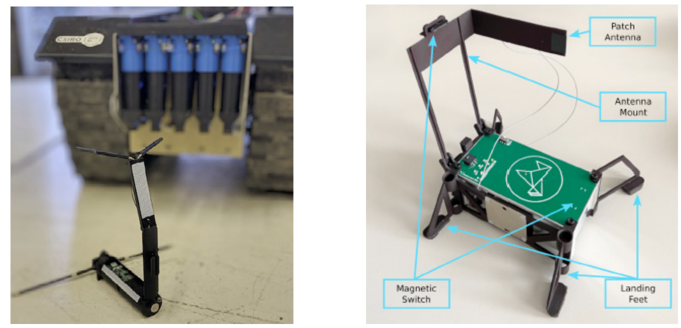

(a) Team CSIRO Data61 (Hudson et al., 2022).

(b) Team CERBERUS (Tranzatto et al., 2022b).

Fig. 2. Spring-loaded Antenna DARPA Breadcrumbs

2.1 *Polarization of Radio Waves*

Polarization of radio waves refers to the orientation of the electric field vector of an electromagnetic wave as it propagates through a medium. An electromagnetic wave originates from a single point and consists of an electric field (E-field) and a magnetic field (H-field). These fields propagate and are orientated as depicted in Fig. 3. The focus of this project is on linear polarization due to the antenna characteristics of ESP32 modules which are used to serve as a proof-of-concept communication device.

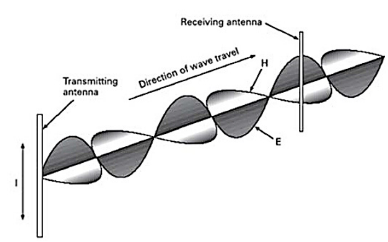

Fig. 3. EM Wave polarized in the Vertical Plane (Dhande, 2009).

Saakian (2020) states that "For real, anisotropic antennas, the radiated electromagnetic field strength at the observation point B depends not just on the distance between communicating points A and B, but also on the antenna's spatial orientation relative to the straight line between those points". In simpler terms, it explains that signal strength depends not only on the distance between the transmitter and receiver antennas, but also on their relative angle.

Furthermore, Zhou et al. (2015) conducted extensive measurements on radio frequency propagation for vertical, horizontal, and cross-polarization in mines and tunnels. It was found that vertically polarized signals attenuated less than horizontally polarized signals in narrow and high tunnels, whereas horizontally polarized signals attenuated less in wide and low tunnels. Thus, it is important to ensure that both transmitting and receiving antennas are of the same polarization mode and are correctly orientated.

3. SYSTEM SPECIFICATIONS

The aim of this project was to develop a proof-of-concept system for communication node deployment on existing Unmanned Ground Vehicle (UGV) platforms. However, to simplify the design specifications and testing procedure, the system was designed specifically for attachment to the Clearpath Husky A200 UGV platform. Thus, the target values for the specifications listed in Table 1 represent best-case scenarios and can be applied to smaller UGV, such as small quadruped robots like Boston Dynamics' Spot robot.

3.1 Design Constraints

The initial step involved determining design constraints to evaluate the final prototype quantitively. These constraints are summarised in Table 1 and were determined by comparison to designs from the DARPA teams. Furthermore, constraints relating to the robustness of the design due to subterranean environmental factors are not provided as it is beyond the scope of the project.

Table 1. Design Constraints.

Description	Target	Range	Unit
Node Deployment System			
Footprint	400	300 - 450	cm^2
Storage Capacity	4	2 - 6	Nodes
Modularity	True	-	-
Mass	3.5	< 5	kg
Self-righting Node System			
Volume	1000	600 - 1200	cm^3
Self-righting Time	20	< 30	s
Node Mass	300	< 500	g
Self-righting Accuracy	98	> 95	%

Ensuring modularity and minimising the form factor and mass of the deployment system are essential constraints for validating the feasibility of the design across various UGV platforms, each with differing spatial and payload requirements. With respect to the Self-righting Node (SRN) system, the two primary constraints were self-righting accuracy and volume. The volume of the node deployment system is directly dependent on the form factor of the SRNs; therefore, minimising it is essential to keep the overall size of the system as small as possible. Self-righting accuracy is defined as the deviation in g-force measurement of the SRN relative to a perfect upright orientation.

3.2 High-level Solution

Following the overall design constraints, a high-level functional decomposition was developed, as illustrated in Fig. 4. The project was divided into subsystems, namely the Node Deployment System and the SRN system. The Node Deployment System was further subdivided into a storage module and a deployment module. This structure enables the system to be modular and scalable to satisfy varying mission requirements.

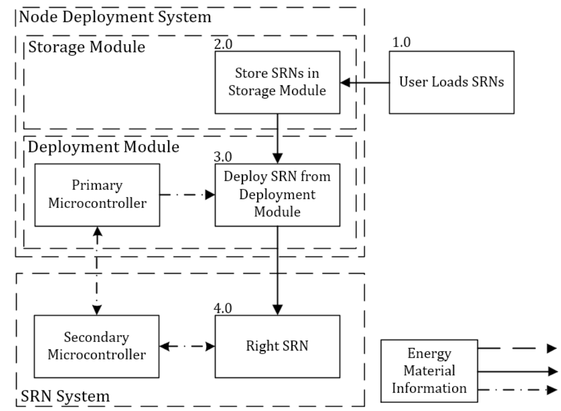

Fig. 4. High-level Functional Decomposition.

4. CONCEPT DESIGN

The design constraints and high-level functional decomposition provided guidance for the concept design phase, during which 3D models were developed using Autodesk Fusion 360. This phase followed an iterative development cycle in which concepts were generated, 3D-printed, tested, and adapted to address any functional or design errors. This approach enabled a time and cost-efficient design process, resulting in the final prototype designs presented in the following section.

5. MECHANICAL SYSTEM DESIGN

Two prototype SRNs were developed, namely the servo-actuated SRN and the gravity-gimbal SRN. The servo-actuated SRN utilizes four micro servo motors, with support legs attached, to self-right the node. This is an active (electronically-actuated) self-righting solution. On the other hand, the gravity-gimbal SRN is a passive self-righting mechanism that utilizes gravity to rotate the gimbal to correctly orientate the antenna inside. To simplify the development of a proof-of-concept SRN, ESP32 microcontrollers were selected, as they have built-in Wi-Fi antennas and functionality that can be used to emulate a sophisticated mesh network. Additionally, the ESP32 microcontrollers provide the General Purpose Input Output (GPIO) pins required to control peripheral devices used in the designs.

5.1 Servo-actuated SRN

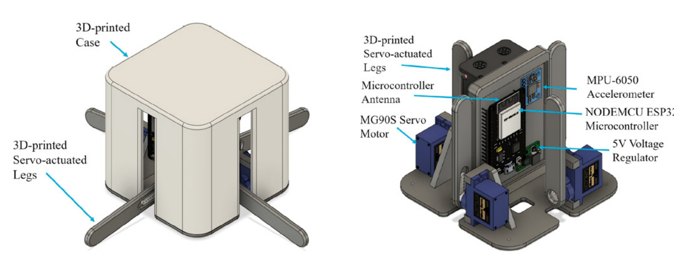

(a) Legs Actuated. (b) Legs Retracted.

Fig. 5. Final Prototype Servo-actuated SRN.

The first prototype design presents the electronic and software-base SRN solution. This design as depicted in

Fig. 5 utilises four servo motors and an accelerometer in a control loop to iteratively adjust the legs attached to the servos until a reading of 1 g is measured on the y-axis of the accelerometer.

5.2 Gravity-gimbal SRN

The second prototype design, shown in Fig. 6, depicts the mechanical-based solution, which draws inspiration from camera stabilisers and gimbals. In this design, the batteries used to power the microcontroller and the accelerometer are positioned lower to offset the centre of mass below the axis of rotation, as defined by the pin joint shown in Fig. 6. This configuration enables the system to remain upright with respect to gravity, regardless of the orientation of the outer protective casing.

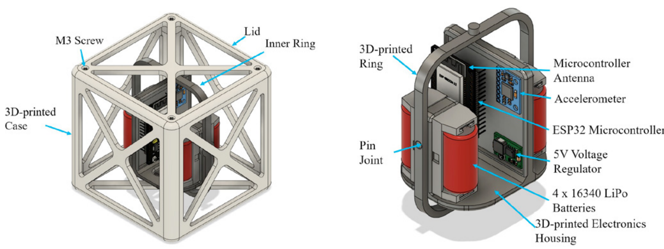

(a) With Case. (b) Without Case.

Fig. 6. Final Prototype gravity-gimbal SRN.

5.3 Deployment Module

The deployment module's outer assembly is constructed from of 20 × 20 mm aluminium extrusions, where the 3D printed parts are placed and fastened. This construction enables the design to be easily reconfigured and adapted throughout the development process. Furthermore, the deployment module houses all the electronics used to dispense SRNs from the UGV, including a small N20 motor with a lead screw attachment to facilitate the dispensing of SRNs from the UGV.

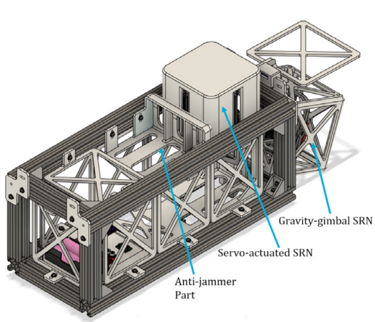

Fig. 7. Deployment System - Deployment Module.

5.4 Storage Module

The storage module, designed to be attached atop the deployment module, is purely mechanical, allowing for scalability. The storage module features a spring-loaded pusher, as depicted in Fig. 8, which ensures that three SRNs can be stored and automatically loaded into the deployment module when empty.

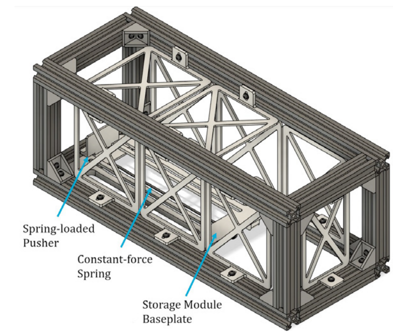

Fig. 8. Deployment System - Storage Module.

6. SOFTWARE AND ELECTRONIC SYSTEM DESIGN

This section details the electrical and software design for the servo-actuated SRN, the gravity-gimbal SRN and the node deployment system. Additionally, a high-level system integration overview is presented which depicts the ESP-NOW communication topology between the microcontrollers in the system. Future work will involve replacing the ESP32 with a communication module more suited for the environment.

6.1 System Integration

The system consists of three distinct ESP32 microcontrollers: one master (primary) and two slave (secondary) microcontrollers. The primary microcontroller, located in the deployment module, is responsible for facilitating two-way communication between itself and the secondary microcontrollers located in the SRNs. Additionally, the primary microcontroller hosts the Control Interface Graphical User Interface (GUI), which sends commands to the primary microcontroller for decoding and transmission to the secondary microcontrollers. This setup is only to validate the performance of the deployment system and the individual SRNs, and not the mesh network performance.

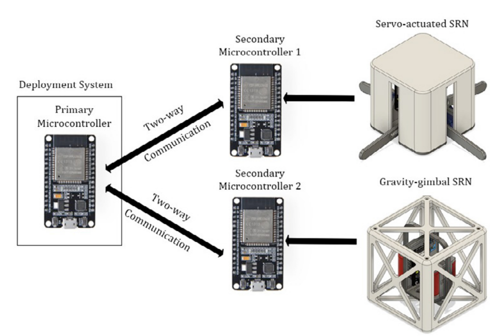

Fig. 9. ESP-NOW Communication Topology.

Secondary microcontroller 1 is responsible for controlling the servo motors in response to commands received from the primary microcontroller. While secondary microcontroller 1 both receives commands and transmits acquired data to the primary microcontroller for publication on the Control Interface GUI, secondary microcontroller 2 only transmits acceleration data, as it is an electronically passive SRN. As a result, secondary microcontroller 1 receives a self-righting command, whereas secondary microcontroller 2 does not require such a command.

7. SYSTEM EXPERIMENT AND ANALYSIS

Following intermediate development tests, field tests were conducted on uneven terrain. These tests involved deploying the communication nodes in various uneven ground topologies to assess the effectiveness of the system in real-world applications. The UGV utilized for this test was the ClearPath Husky A200 platform.

7.1 Self-righting Node Experiment

Fig. 10 and Fig. 11 show the acceleration versus time responses for the deployment of both SRN designs. These plots correspond to one of the five experiments listed in Table 2 and represent the independent testing of each SRN design. The data in Fig. 10 is clipped to the moment the self-righting command is received, whereas Fig. 11 captures the point at which the gravity-gimbal SRN makes contact with the ground and begins self-righting. The experiment involved loading one of the SRN designs into the deployment module and dispensing it five times to measure the self-righting time and steady-state y-axis (vertical) acceleration values, before swapping to the other design and repeating the procedure.

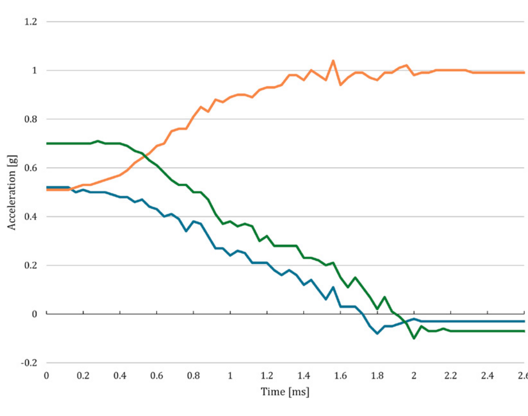

Fig. 10. Acceleration vs Time - Servo-actuated SRN.

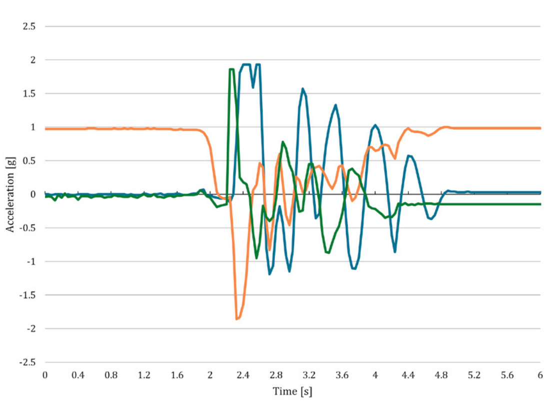

Fig. 11. Acceleration vs Time - Gravity-gimbal SRN.

It is seen in Fig. 10 that the servo-actuated SRN algorithm correctly identified the nodes orientation after deployment and began to adjust the servo motors until a g-force value of 1 g was measured for the y-axis. While the gravity-gimble SRN produced an oscillatory response due to the two axis of rotational freedom.

Table 2. Average of SRN Experiment Results.

SRN Type	Self-righting Time (s)	Steady-state y-axis g-force (g)
Servo-actuated	1.90	0.99
Gravity-gimbal	2.86	0.97

The servo-actuated SRN algorithm is effective in making live adjustments, ensuring that the node rights itself, even in the presence of minor disturbances, such as slipping caused by the legs pressing against soil or loose rock. A limitation of the gravity-gimbal SRN is the friction in the joints, which produces a linearly-damped decay response. While this characteristic offers advantages in reducing the self-righting time, it can cause the system to stop in an unsuitable orientation due to static friction overcoming the angular inertia, thus resulting in the steady-state g-force error seen in Table 2. However, using a material with a lower coefficient of friction will improve the accuracy of the steady-state y-axis g-force but will increase the self-righting time due to less damping and frictional forces present. Click *here* to view a video summary of the project.

7.2 Field Test

The field test was conducted outside on rough terrain with the deployment system mounted to the Husky A200 UGV. Fig. 12, depicts the deployment and final steady-state orientation of the servo-actuated SRN.

(a) Deploying SRN. (b) Successful Deployment.

Fig. 12. Field Test.

Several outdoor tests were conducted, the first being validating the success of the nodes' self-righting functionality by deploying each node independently. Following the SRN tests, the node deployment system was tested by deploying one node, then two and three nodes sequentially. Thereby testing the reliability of the storage system to reload the deployment module when empty. The results of these tests are summarised in Table 3 below.

Table 3. Field Test Results.

Description	Target	Range	Result	Unit
Node Deployment System				
Footprint	400	300–450	555	cm^2
Storage Capacity	4	2–6	3	Nodes
Modularity	True	-	True	–
Mass	3.5	<5	3.1	kg
Servo-Actuated SRN				
Volume	1000	600–1200	855.03	cm^3
Self-Righting Time	20	<30	1.90	s
Node Mass	300	<500	360	g
Self-Righting Accuracy	98	>95	99	%
Gravity-Gimbal SRN				
Volume	1000	600–1200	1168.54	cm^3
Self-Righting Time	20	<30	2.86	s
Node Mass	300	<500	260	g
Self-Righting Accuracy	98	>95	97	%

Additionally, battery life values for the respective subsystems were determined mathematically. The node deployment system is powered using two 18650 lithium-ion batteries, providing a total capacity of 4400 mA h, corresponding to 16.8 hours of battery life. The servo-actuated SRN is powered using batteries of the same capacity; however, due to the holding torque required to maintain the node in an upright position, there is an increased current draw, which reduces the battery life of the node to 8 hours. The gravity-gimbal SRN is powered using four 16340 lithium-ion batteries, resulting in a total capacity of 2800 mA h. Although the gravity-gimbal SRN has a considerably lower battery capacity, it exhibits a longer battery life of 12.3 hours because it only requires power for the ESP32 microcontroller and the accelerometer.

8. CONCLUSION AND FUTURE WORK

A proof-of-concept deployment system was successfully developed to establish mesh communication infrastructure. Two distinct self-righting communication node designs were developed, tested, and quantitatively analysed. Both designs satisfied the design constraints; however, it was noted that for future development, the servo-actuated SRN is the preferred design. This preference arises due to scalability limitations present in the gravity-gimbal SRN. If a more sophisticated communication device is to be utilised, typically occupying a larger form factor, the size of the gravity-gimbal SRN would increase considerably, rendering it impractical for use on small UGVs. Additionally, the servo-actuated SRN offers several advantages, including user control over its orientation and the ease with which servo mechanisms and algorithms can be implemented without significantly increasing the overall form factor.

Future development should focus on advancing the design of the servo-actuated SRN and the node deployment system to enhance their robustness against hazardous environments. Furthermore, implementing the servo-actuation mechanism and algorithms on an off-the-shelf communication device is recommended. While the ESP32 modules served effectively as simulated mesh network nodes and peripheral control devices, future research should involve comprehensive testing of commercially available hardware using various communication protocols such as WiFi, Zigbee, and LoRa within realistic mesh network topologies and environments. This will help determine the most suitable hardware and protocol combinations for different application scenarios. In terms of node deployment location decision-making, greedy algorithms based on RSSI thresholding should be investigated in conjunction with the solutions presented in this report.

ACKNOWLEDGEMENTS

The authors would like to thank Enaex Africa for funding this project.

REFERENCES

Candido, B., Santos, N., Moutinho, A., and Zacchi, J. (2025). Uncrewed ground vehicles in military operations: Lessons learned from experimental exercises. In A. Pereira, A. Lopes, E. Pedrosa, J. Lima, P. Fonseca, T. Meireles, and V. Pinto (eds.), *2025 IEEE International Conference on Autonomous Robot Systems and Competitions, ICARSC 2025*, 21–26. Institute of Electrical and Electronics Engineers Inc., United States. DOI: 10.1109/ICARSC65809.2025.10970121.

Cruz-Ausejo, L. et al. (2024). Occupational accidents in mining workers: scoping review of studies published in the last 13 years. *BMJ open*. DOI: 10.1136/bmjopen-2023-080572.

Dhande, P. (2009). Antennas and its Applications. *DRDO Science Spectrum*, 66–78.

Hudson, N., Talbot, F., Cox, M., Williams, J., Hines, T., Pitt, A., Wood, B., Frousheger, D., et al. (2022). Heterogeneous ground and air platforms, homogeneous sensing: Team csiro data61's approach to the darpa subterranean challenge. *Field Robotics*, 2, 595–636. DOI: 10.55417/fr.2022021.

Saakian, A. (2020). *Radio Wave Propagation Fundamentals*. Artech House, 2nd edition.

Tatum, M. (2020). Communications Coverage in Unknown Underground Environments. Unpublished Thesis. Carnegie Mellon University.

Tranzatto, M., Dharmadhikari, M., Bernreiter, L., Camurri, M., Khattak, S., Mascarich, F., Pfreundschuh, P., Wisth, D., et al. (2022a). Team CERBERUS Wins the DARPA Subterranean Challenge: Technical Overview and Lessons Learned. DOI: 10.48550/arXiv.2207.04914.

Tranzatto, M., Miki, T., Dharmadhikari, M., Bernreiter, L., Kulkarni, M., Mascarich, F., Andersson, O., Khattak, S., et al. (2022b). Cerberus in the darpa subterranean challenge. *Science Robotics*, 7. DOI: 10.1126/scirobotics.abp9742.

Zhou, C., Plass, T., Jacksha, R., and Waynert, J. (2015). RF Propagation in Mines and Tunnels. *IEEE Antennas and Propagation Magazine*, 57, 88–102. DOI: 10.1109/MAP.2015.2453881.